The object of the study is a capacitor exciter with variable topology, designed to operate as part of an autonomous induction generator. Insufficient efficiency of controlling the excitation level of an autonomous induction generator when changing the speed of the drive turbine and the load impedance has been established. This reduces the quality of the generator output voltage. The possibility of using an exciter circuit based on a mixed connection of capacitors has been analyzed. The influence significance of the groups number and the number of capacitors in each group on the range width and the adjustment step has been confirmed. In particular, increasing the values of the specified factors from 2 to 4 expands the adjustment range by 16 times, and the number of steps by 827 times. With the selected intervals of factors variation and a significance level of 0.05, the influence of the capacitors value changing step, compared to the base one, on the relative value of the exciter capacitance changing step is recognized as insignificant. The total capacitance of the exciter depends significantly nonlinearly on the number of the topological state. An increase in the total capacitance is accompanied by a raising in the intensity of its growth. This allows to minimize the step change in the total capacitance (with a probability of 0.88 – up to 0.003 % of the control range width). The resulting regression mathematical model can be used to optimize the exciter structure for an autonomous induction generator of a specific type. Increasing the number of control stages will enhance the accuracy of forming the capacitive excitation current of the generator and compensating the load current inductive component. The use of an exciter with a variable topology will increase the efficiency of voltage control of an autonomous induction generator when changing the speed of the drive turbine and the load impedance

Keywords: induction generator, capacitor exciter, autonomous power grid, voltage quality, reactive power, microgrid

UDC 621.313.332
DOI: 10.15587/1729-4061.2025.326178

DETERMINATION OF REGULATION CHARACTERISTICS OF CAPACITOR EXCITER WITH VARIABLE TOPOLOGY FOR SELF-EXCITED INDUCTION GENERATOR

Sviatoslav Vasylets
Corresponding author
Doctor of Technical Sciences, Professor*
E-mail: svyat.vasilets@gmail.com
Kateryna Vasylets
PhD, Associate Professor*
Volodymyr Ilchuk
Senior Lecturer*
*Department of Automation, Electrical Engineering and Computer-Integrated Technologies
National University of Water and Environmental Engineering
Soborna str., 11, Rivne, Ukraine, 33028

Received 03.01.2025
Received in revised form 14.03.2025
Accepted 31.03.2025
Published 21.04.2025

How to Cite: *Vasylets, S., Vasylets, K., Ilchuk, V. (2025). Determination of regulation characteristics of capacitor exciter with variable topology for self-excited induction generator. Eastern-European Journal of Enterprise Technologies, 2 (8 (134)), 17–25. https://doi.org/10.15587/1729-4061.2025.326178*

1. Introduction

The European Green Deal envisages the achievement of climate neutrality by the European Union countries by 2050 [1]. This goal is specified in the package of legislative initiatives "Fit for 55", which is to reduce greenhouse gas emissions by 55 % by 2030 through implementing a set of measures, in particular, in the energy sector. More than 145 countries have announced their intentions to reduce CO_2 emissions between 2050 and 2070, such as, China by 2060, India by 2070 [2]. One of the main ways to achieve this goal is to replace fossil fuel energy with renewable sources. This also increases the energy independence of countries. In 2022, against the backdrop of the Russian invasion of Ukraine, the EU adopted the REPowerEU plan [3]. It envisages expanding the use of electricity in various industries, in transport, and replacing fossil fuels with renewable sources. According to the European Commission's plan for the digitalization of the energy system, the infrastructure of smart grids should be improved by creating a European Energy Data Space [4]. Investments in the electricity sector are estimated at 584 billion euros over the period 2020–2030, which will allow increasing the share of renewable sources in the energy balance. Compared to 13 % in 2023, this indicator should reach 20 % in 7 years [5]. By 2030, the installed capacity of onshore wind farms is expected to double to 846 GW. The capacity of offshore wind farms should reach 212 GW [6]. The development of renewable energy sources is extremely important for Ukraine due to damage to power facilities as a result of hostilities [7]. The "Energy Strategy of Ukraine for the period until 2050" provides for an increase in the capacity of renewable sources, in particular, wind generation up to 140 GW, and hydrogeneration – up to 9 GW [8].

One of the common types of generators, that wind power plants, small hydroelectric power plants and cogeneration plants are equipped with, is an induction generator (IG). Induction generators are widely used in wind power plants with a capacity of up to several MW [9]. In particular, the Saint-Rémy-des-Landes wind turbine (manufacturer GEC-ALSTHOM NEYRPIC, France) with a capacity of 1000 kW is equipped with an IG of 3 kV nominal output voltage. The MWT-62/1000A wind turbine (Mitsubishi, Japan) of similar capacity is equipped with an induction generator of 600 V output voltage. The global IG market volume for 2023 is estimated at 1.96 billion USD. At an average annual growth rate of 7 %, it should reach

2.63 billion USD by 2030 [10]. IGs are characterized by high reliability indicators. In particular, as a result of the analysis of 1.44 million hours of operation of 76 wind generators, which belongs to megawatt power range, as a part of four wind farms in China, 423 failures were identified, including 112 emergency situations [11]. 43 % of failures occurred in the electrical part of the wind turbine: 78 failures occurred due to the generator, 104 – electrical equipment.

The ability of IG to operate in network and autonomous modes is consistent with the implementation of the microgrid concept [12]. One of the main disadvantages of autonomous IG is the need for a source of reactive capacitive power for self-excitation of the generator and compensation of reactive inductive power of the load. The limited range of capacitance regulation, which is typical for excitation schemes, the use of semiconductor converters to regulate the capacitive excitation current or the generator output voltage reduce the quality of the latter [13]. Significant disturbances for IG are the stochastic change in the rotor speed and load impedance [13], which negatively affect the stability of the frequency and amplitude of the generator voltage.

Thus, the need to stabilize the operating parameters of an induction generator as part of an autonomous power supply system determines the relevance of the disclosed scientific issues.

2. Literature review and problem statement

Excitation of an autonomous IG with one stator winding and a squirrel cage rotor is carried out by a parallel three-phase capacitor [14]. The drawback is the dependence of the output voltage parameters on the nature of the motor magnetization curve, the speed of the wind- or hydroturbine rotor, and the load power. To partially compensate for the influence of the latter factor, it is possible to implement mixed self-excitation when additional series (compound) capacitors are connected [15]. This method expands the range of self-excitation of IG, but the critical values of the compound capacitances limit the lower bound of the control range.

Semiconductor converters can be used to regulate the magnitude of the capacitive excitation current. Control of the power switches of the static synchronous compensator STATCOM can be performed using genetic, firefly algorithms or an adaptive neuro fuzzy inference system [16]. However, such a compensator does not provide high control quality indicators in dynamic modes.

Partially, the IG disadvantages can be overcome by constructive measures. The stator windings of a dual star induction generator are made of two parallel branches, between which there is a spatial shift (most often 20–40°). Loads with a reactive power compensator are connected to one of the half-windings, and excitation capacitors to the other. The output voltage of the dual star IG can be regulated using a semiconductor converter with a DC link [17]. However, this method causes generator torque pulsations and higher harmonics in the current curve. To reduce such negative phenomena, direct vector torque control based on space vector modulation is used [18]. But the mutual inductive coupling of the IG half-windings negatively affects the static and dynamic properties. It is proposed to improve the control quality and stability of the dual star IG in a wind turbine when the wind speed changes by using a controller based on fuzzy logic [19]. However, such a solution requires a complex tuning procedure.

To improve the IG operational characteristics, doubly-fed generators were developed, which are an induction machine with a wound rotor. The latter is connected to the network through a semiconductor back-to-back converter. By changing the rotor operating mode, it is possible to stabilize the generator output voltage [20]. However, the issue of ensuring stability and desired quality indicators, especially in transient modes, has not been fully resolved [21]. The random nature of the wind speed change leads to fluctuations in the frequency of the output voltage of doubly-fed IG. There is a known proposal to apply two control strategies for such an electric machine: frequency smooth control and dynamic inertial [22]. The transition between strategies is proposed to be carried out by a smooth switch that uses an integrator to avoid step changes in the generator coordinates in transient modes. However, with this approach, difficulties arise in maintaining the required dynamic control accuracy. In circuits with doubly-fed IG compound capacitors may be utilized [23]. The disadvantages of this approach include the possibility of problems with subsynchronous resonance.

Literature analysis [14–23] allows to establish the existing problem: insufficient efficiency of controlling the excitation level of an autonomous induction generator when changing the speed of the drive turbine and the load impedance. This leads to a decrease in the quality of the generator output voltage. In particular, amplitude and frequency fluctuations occur, which has a negative impact on the functioning of consumers in the autonomous power grid.

3. The aim and objectives of the study

The aim of the study is to increase the efficiency of the capacitor exciter for an autonomous induction generator by discretely adjusting the capacitance by changing the topology of the exciter circuit. This will allow to adjust the reactive power consumed by the generator when changing the rotor speed and the level of electrical load. As a result, generator output voltage quality will be improved, since its amplitude and frequency will be stabilized.

To achieve the aim, the following tasks must be solved:

– to estimate the parameters values of the mathematical model of a capacitor exciter with a variable topology;

– to determine the operating characteristics of the exciter.

4. Materials and methods

4. 1. Object and hypothesis of the study

The object of the study is a capacitor exciter with variable topology, designed to operate as part of an autonomous induction generator. The exciter is based on the discrete principle of changing the total capacitance by switching capacitors of a mixed connection. Each phase of the exciter includes m groups of capacitors, Fig. 1. The $i=1...m$ group includes p_i capacitors $C_{i,1},\ldots,C_{i,p_i}$, which are connected in parallel within the group. Each capacitor is shunted by a discharge resistor $R_{i,1},\ldots,R_{i,p_i}$. Each capacitor with the corresponding resistor is commutated within the group by a switch $S_{i,j}$, $j=1,\ldots,p_i$ (for example, of a semiconductor type). The closed state of the switch corresponds to logical "1", the open state corresponds to "0". The groups can be connected in series or in parallel, which is provided by switchboards $K_1,\ldots,K_{m-1}$. Each such switchboard includes three switches $K_{r,1}$, $K_{r,2}$ and

$K_{r,3}$, $r=1,\ldots,m-1$. The parallel connection of groups adjacent to the switchboard K_r, denoted by $K_r=0$, corresponds to the following state of switches: $K_{r,1}=1$; $K_{r,2}=0$; $K_{r,3}=1$. When the groups are connected in series ($K_r=1$), the state of the switches of the r-th switchboard is inverted. The three-phase exciter includes three symmetrical phases, Fig. 1, connected according to the delta scheme.

The subject of the study is the process of discrete regulation of the capacitance of the capacitor exciter. Regulation is carried out by changing the number of connected capacitors and their connection scheme. Since the total number of switches of one phase of the capacitor exciter is:

$$g = m - 1 + \sum_{i=1}^{m} p_i, \tag{1}$$

then the total number of states is:

$$N = 2^g. \tag{2}$$

However, from this number it is necessary to exclude N' states, which correspond to the violation of the electrical connection between the terminals L and T of the exciter phase. It is also necessary to avoid cases of repetition of the values of the phase capacitances, let's denote the number of such states N''. Then the total number of permissible states of the capacitor exciter is $H=N-N'-N''$.

The main hypothesis of the study is the possibility of minimizing the mean $\overline{\delta}$, in percent of the control range width, of the step change in the exciter capacitance. In this case, the condition must be met:

$$\overline{\delta} \le \delta', \tag{3}$$

where $\delta'=0.2$ % is the largest permissible value of δ accepted in this study.

The value $\overline{\delta}$ is defined as:

$$\overline{\delta} = m[\delta], \tag{4}$$

where δ is the relative step of change in the exciter capacitance:

$$\delta = \frac{C_\Delta}{C_{\max} - C_{\min}} \cdot 100\%, \tag{5}$$

where C_Δ is the absolute value of the step change in the exciter capacitance; $C_{\max}$, $C_{\min}$ are the endpoints of the control range.

It is assumed that the capacitances of each of the following capacitors increase by the value $\Delta C>0$, relative to the capacitance of the base $C_{1,1}$.

4. 2. Algorithm and computer program for determining permissible states of a capacitor exciter

The initial data for determining the permissible states of the capacitor exciter are the total number of capacitor groups m, the number and capacitance of capacitors in each group, Fig. 2, block 2. The total number of switch states is calculated in accordance with (1) and (2), block 3. The main program cycle (blocks 4–23) involves calculating the total capacitance of the exciter phase $C_\Sigma^{[k]}$ for each $k=\overline{0,N-1}$ of the possible states.

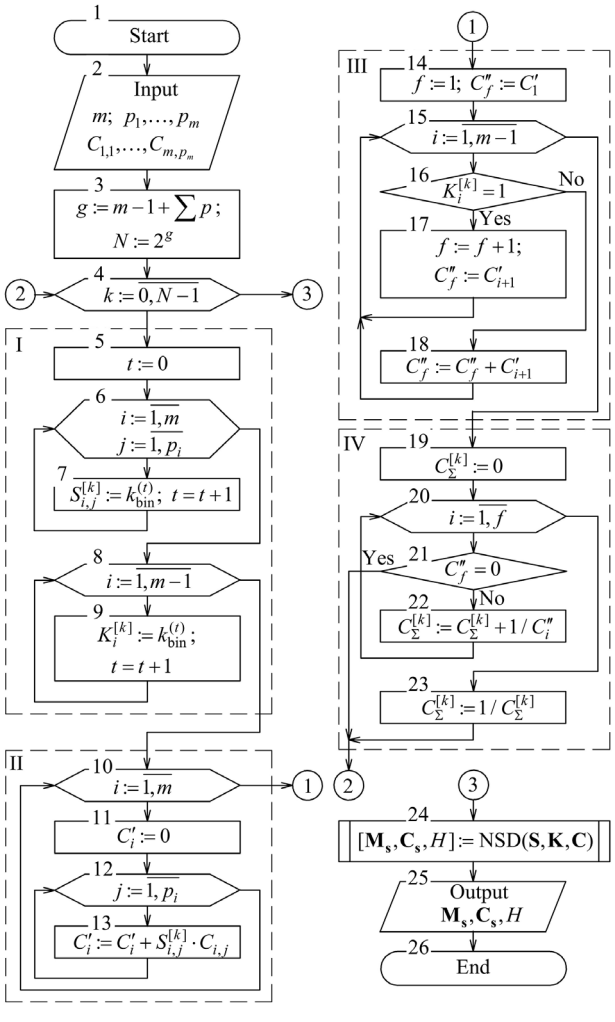

Fig. 2. Flowchart of the algorithm for determining the permissible states of the capacitor exciter

Module I in the main cycle (blocks 5–9) is intended to determine the state of the switches and switchboards, which corresponds to the current number k of the exciter state, Table 1.

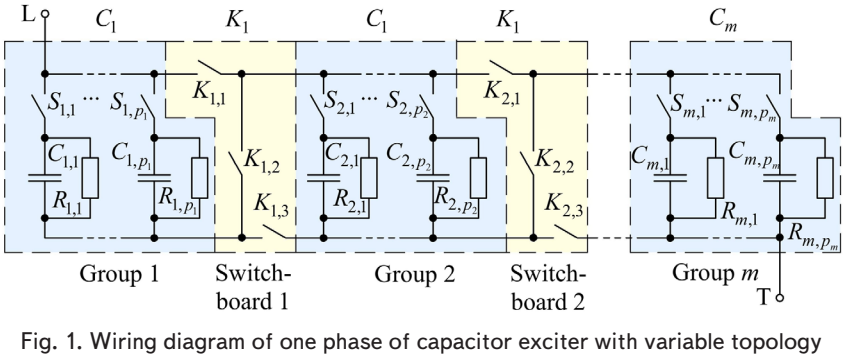

Fig. 1. Wiring diagram of one phase of capacitor exciter with variable topology

Table 1

Correspondence of bits of the number k binary representation of the exciter state to the state variables of the switches of capacitor groups and intergroup switchboards

Bit number k	g	...	$1+\sum_{i=1}^{m} p_i$	$\sum_{i=1}^{m} p_i$	...	p_1+p_2	...	p_1+1	p_1	...	0
State of switch/switchboard	K_{1-m}	...	K_1	S_{m,p_m}	...	S_{2,p_2}	...	$S_{2,1}$	S_{1,p_1}	...	$S_{1,1}$

In the cycle (block 6) for groups i and switches in each group j, the values $k_{bin}^{(t)}$ of successive bits of the binary representation of the number k of the exciter state are stored into the three-dimensional matrix S, block 7. Herewith the current bit number is determined by the temporary variable t (block 5), which is incremented in the cycle. After that, in the cycle by the switchboard numbers (block 8), the matrix K is formed by reading the following bits $k_{bin}^{(t)}$ (block 9), and the increment of the variable t continues from the previous cycle. Blocks 10–13 (module II) calculate the capacitances C' of the capacitor groups taking into account the state of the switches. Blocks 14–18 (module III) calculate the equivalent capacitances C'' for groups of capacitors, which, according to the state of the intergroup switchboards, are connected in parallel. The resulting equivalent capacitances in number of f are connected in series. Their total capacitance $C_{\Sigma}^{[k]}$, which corresponds to the exciter phase capacitance, is calculated by blocks 19–23 of module IV.

In the main cycle, a vector C of total capacitances is formed. Zero elements of such a vector correspond to the absence of an electrical connection between the terminals L and T of the exciter phase. A matrix S of the states of the capacitor group switches and a matrix K of the switchboard's states are also formed. Such values are input to the NSD (Non-zero, Sort, Duplicate) subroutine, block 24, which performs three operations. First, it rejects states in number of N' for which the phase capacitance is zero. Second, it sorts non-zero capacitances in ascending order. Third, it removes duplicate N'' values of capacitances. As a result, a matrix M_s of the switches and switchboards states, a matrix C_s of the corresponding exciter phase capacitances are formed, and the number H of permissible states is determined, block 25.

The above algorithm is implemented in the form of a computer program CEVT (Capacitive Exciter with Variable Topology) for determining the permissible states of a capacitor exciter with variable topology, Fig. 3.

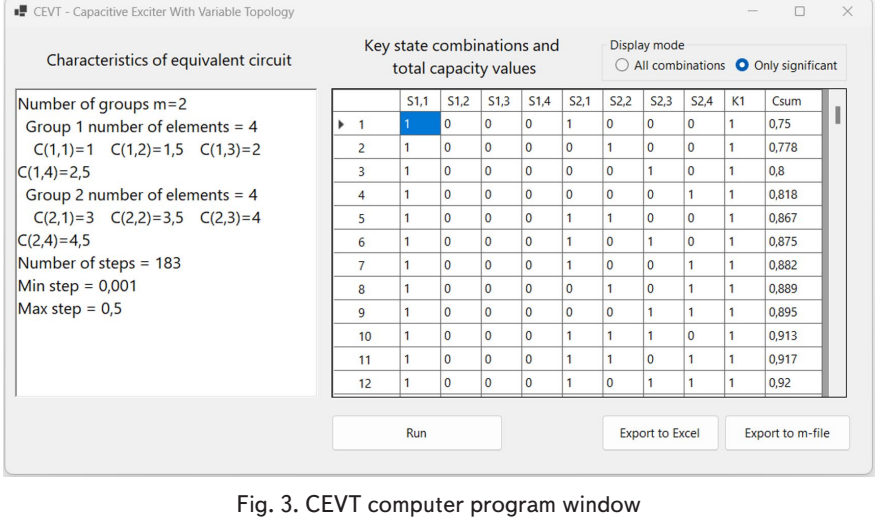

Fig. 3. CEVT computer program window

The program was developed in the Microsoft Visual Studio environment (Microsoft Corporation, USA) using the VB.NET language.

The program reads the input data (number of groups, number and capacitance of capacitors in each group) from the xml file. The left field, Fig. 3, displays the characteristics of the equivalent circuit and the number of permissible exciter states. The table on the right side of the window displays the possible switch states.

4. 3. Planning a numerical experiment to estimate the parameters values of the mathematical model of the exciter

The experiment is carried out assuming the same number of capacitors in each group: $p=p_1=p_2=...=p_m$. The influence of three factors on the exciter is considered, Table 2: x_1 – number of capacitor groups (corresponds to m); x_2 – number of capacitors in each group (p); x_3 – step of changing the capacitances of adjacent capacitors (ΔC, μF). For each factor, the main level (when encoding levels corresponds to 0) and the variation interval I were determined. This made it possible to determine the upper and lower levels of each factor (in the encoded representation +1 and −1, respectively). The value $\overline{\delta}$ (4) was chosen as the objective function.

Table 2

Levels and intervals of factors variation

Exciter parameters	Factors	Factor levels			Variation interval I
		−1	0	+1	
m	x_1	2	3	4	1
p	x_2	2	3	4	1
ΔC	x_3	0.5	1	1.5	0.5

Since there is no a priori information about the nature of the influence of factors and the effects of their interaction, it is planned to assess the significance of the coefficients of the following mathematical model of the exciter:

$$\overline{\delta} = b_0 + b_1x_1 + b_2x_2 + b_3x_3 + b_{12}x_1x_2 + b_{13}x_1x_3 + b_{23}x_2x_3 + b_{123}x_1x_2x_3. \quad (6)$$

This model takes into account the influence of individual factors and their combinations. The estimation of the coefficients' values of model (6) is carried out on the basis of a full factorial experiment of type 2^3 with

a central point, Table 3. In this case, the capacitance of the base capacitor $C_{1,1}$ is taken to be 1 μF.

Table 3

Design matrix for a full factorial experiment of type 2^3 with a central point

Experiment No.	x_1 value		x_2 value		x_3 value	
	coded	natural	coded	natural	coded	natural
1	−1	2	−1	2	−1	0.5
2	1	4	−1	2	−1	0.5
3	−1	2	1	4	−1	0.5
4	1	4	1	4	−1	0.5
5	−1	2	−1	2	1	1.5
6	1	4	−1	2	1	1.5
7	−1	2	1	4	1	1.5
8	1	4	1	4	1	1.5
9	0	3	0	3	0	1.0

For numerical estimation of the coefficients b values of the model (6), the 'fitlm' function is used, available in the MATLAB system (The MathWorks, USA). The function performs regression of the empirical values obtained as a result of a numerical experiment. The analysis of variance of the regression model is performed using the 'anova' function. In this case, the significance level is taken as $\alpha=0.05$.

5. Results of the study of discrete exciter capacitance control

5. 1. Estimates of the parameters' values of the exciter mathematical model

As a result of performing a full factorial numerical experiment, the values of the main parameters of the capacitor exciter were obtained. The values of the objective function $\overline{\delta}$ were calculated using (5), Table 4.

Performing the regression of $\overline{\delta}$ empirical values made it possible to obtain estimates of the model (6) coefficients, the value of the standard error and asymptotic significance (p-value), Table 5. The regression is characterized by the following indicators: the mean squared error of the regression is 0.986, the coefficient of determination is 0.9, and the adjusted coefficient of determination is 0.725.

Table 4

Results of a full factorial numerical experiment to estimate the parameters values of the exciter mathematical model

Exciter parameter	Experiment No.								
	1	2	3	4	5	6	7	8	9
H	20	518	183	7084	22	796	278	18209	498
$\max[C_\Delta]$, μF	0.5000	0.5000	0.5000	0.5000	1.5000	1.5000	1.5000	1.5	1
$\min[C_\Delta]$, μF	0.0140	0.0010	0.0010	0.0010	0.0460	0.0010	0.0010	0.0010	0.0010
$m[C_\Delta]$, μF	0.2807	0.0397	0.1113	0.0105	0.5333	0.0608	0.1737	0.0107	0.0871
C_{max}, μF	6	21	21	75	12	49	49	195	44
C_{min}, μF	0.6670	0.4800	0.7500	0.5970	0.8000	0.6700	0.8750	0.7860	0.7180
$\overline{\delta}$, %	5.2632	0.1934	0.5495	0.0141	4.7619	0.1258	0.3610	0.0055	0.1996

Table 5

Results of numerical estimation of the coefficients b values of model (6) by regression of empirical values

Model coefficient	Coefficient estimates	Standard error	p-value
b_0	1.0066	0.2848	0.0241
b_1	−1.3246	0.3488	0.0191
b_2	−1.1768		0.0279
b_3	−0.0958		0.7973
b_{12}	1.1019		0.0342
b_{13}	0.0767		0.8367
b_{23}	0.0465		0.9004
b_{123}	−0.0317		0.9319

In model (6), components can be discarded for which coefficients have asymptotic significance $p>\alpha$. For such coefficients, at the adopted significance level $\alpha=0.05$, the null hypothesis of a zero value is not rejected by the two-sided t-test. Then the mathematical model of the exciter in the coded factors values has the form:

$$\overline{\delta} = b_0 + b_1 x_1 + b_2 x_2 + b_{12} x_1 x_2. \quad (7)$$

The results of the analysis of variance (ANOVA) of the regression model (7) are presented by the estimates of the sum of squared deviations, the mean square, the F-test and its asymptotic significance, Table 6.

Table 6

Results of the analysis of variance of the regression model (7)

Type of variance	Sum of squares	Degrees of freedom	Mean square	F-statistic value	p-value
Total	38.8657	11	3.5332	–	–
Model:	34.8279	3	11.6093	23.0015	$2.7449\cdot10^{-4}$
– linear	25.1149	2	12.5575	24.8801	$3.6800\cdot10^{-4}$
– nonlinear	9.7130	1	9.7130	19.2444	0.0023
Residual:	4.0378	8	0.5047	–	–
– lack of fit	3.8920	1	3.8920	186.9379	$2.6372\cdot10^{-6}$
– pure error	0.1457	7	0.0208	–	–

Such indicators are determined for the factorial (intergroup) variance, which arises under the influence of two significant factors. The influence of the linear and nonlinear parts of the model (7) is estimated separately. Also listed are the indicators determined for the residual (intragroup) variance, which is specified by random factors that were not taken into account by the model. For the residual variance, the influence of the model imperfection and the influence of the experimental error are distinguished. The mathematical model (7) with the natural values of the factors is as follows:

$$\overline{\delta} = a_0 + a_1 m + a_2 p + a_{12} mp, \quad (8)$$

where $a_0=18.4279$, $a_1=-4.6303$, $a_2=-4.4825$, $a_{12}=1.1019$ are estimates of the model coefficients.

The transition from coded to natural values of factors was carried out taking into account the natural values of the main level of factors and variation intervals, Table 2.

5. 2. Determination of the regulation characteristics of the exciter

For the conditions of experiments 1–8, the regulation characteristics of the capacitor exciter were obtained, Fig. 4. These are the dependences of the total capacitance C_Σ of the exciter phase on the exciter state number ζ. The states are numbered in ascending order by C_Σ.

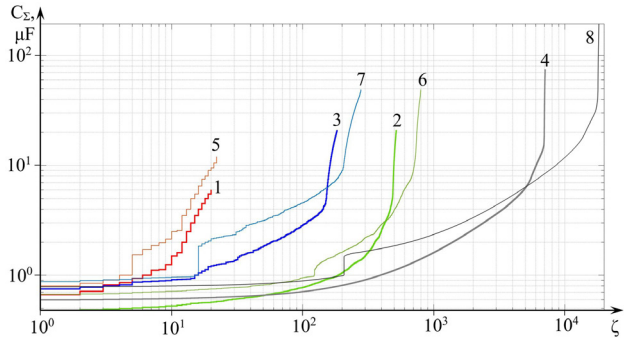

Fig. 4. Regulation characteristics of the capacitor exciter for the conditions of experiments 1–8, plotted on a logarithmic scale, the curve number corresponds to the experiment number

The step characteristics of the capacitor exciter were obtained, Fig. 5.

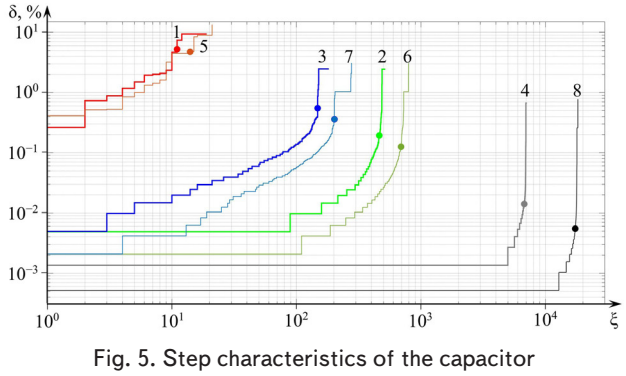

Fig. 5. Step characteristics of the capacitor exciter in experiments 1–8, plotted on a logarithmic scale, the curve number corresponds to the experiment number, the dots indicate $\overline{\delta}$ mean

Step characteristics are the dependences of the relative step δ of the change in exciter capacitance on the number ξ of the exciter state. The states are numbered in ascending order by δ.

6. Discussion of the results of the study of discrete exciter capacitance control

Analyzing the results of the full factorial experiment (Table 4), it is possible to establish a significant influence of the number of capacitor groups m (factor x_1) and the number p of capacitors in each group (factor x_2) on the exciter parameters. An increase in m and p significantly increases the total number H of permissible exciter states and the upper endpoint C_{max} of the control range. In particular, at $m=2$, $p=2$ (experiment 1) $H=20$, and at $m=4$, $p=4$ (experiment 4) $H=7084$, i.e. there is an increase in H by 354 times. The increase in C_{max} is 13 times. In experiment 8, compared to experiment 5, H increased by 827 times, C_{max} by 16 times. However, such a significant increase is not observed when changing the value of ΔC (factor x_3): between experiments 4 and 8 H increased only by 2.5 times, C_{max} by 2.6 times. Also, increasing m and p significantly reduces the mean $m[C_\Delta]$ of the absolute step change in the exciter capacitance and the value of $\overline{\delta}$. In experiment 4, compared to experiment 1, there is a decrease $\overline{\delta}$ of 373 times, in experiment 8, compared to 5, – 866 times. The lower endpoint C_{min} of the control range and the minimum value of the step $\min[C_\Delta]$ of the capacitance change in all experiments remain practically unchanged. The value of the maximum step $\max[C_\Delta]$ of the exciter capacitance change is equal to the value ΔC of the change in the capacitances of adjacent capacitors. The coefficients of the mathematical model (6) were estimated by regression analysis, Table 5. The values of the coefficient of determination of 0.9 and the adjusted coefficient of determination of 0.725 indicate sufficient accuracy of the regression [24]. The asymptotic significance p for the coefficients b_3, b_{13}, b_{23}, b_{123} of the model significantly exceeds the accepted level of significance $\alpha=0.05$. This, according to the Student's t-test, indicates the insignificance of the corresponding model components. From this it can be established that the factor x_3 (the value of ΔC) does not have a significant impact on the objective function either independently or in interaction with other factors. After excluding the insignificant factor x_3, the mathematical model (7) of the exciter includes a constant component and components due to the separate influence of x_1, x_2 and their interaction $x_1 \cdot x_2$. Based on the variance analysis of the regression model (7), Table 6, it was established that the main contribution to the total sum of squared deviations (38.8657) is made by the factor variance, for which the corresponding value is 34.8279. The asymptotic significance of the factor (intergroup) variance ($p=2.7449\cdot10^{-4}$) is significantly less than the accepted significance level α. This confirms the significant influence of the factors x_1, x_2 on the objective function. The value of the F-test for the linear component of the factor variance (24.8801) exceeds the nonlinear component (19.2444). This indicates the predominance of the influence of factors x_1 and x_2 on the objective function over the influence of their interaction $x_1 \cdot x_2$. Interpreting model (7), it is possible to establish the measure of the influence of each of the factors on the objective function. Since $b_1<0$ and $b_2<0$, with an increase in the values of factors x_1, x_2 the value $\overline{\delta}$ decreases. The absolute value of the estimate $|b_1|$ exceeds $|b_2|$, which indicates the predominance of the influence of factor x_1 on the objective function over the influence of x_2. That is, an increase in the number of capacitor groups provides a more intensive reduction in the mean step of the exciter capacitance change than an increase in the number of capacitors in the groups. However, such $\overline{\delta}$ reduction is somewhat limited by the component of the interaction of factors $x_1 \cdot x_2$, the coefficient at which $b_{12}>0$. Such trends are preserved when moving to model (8) in the full-scale values of the factors.

The insignificance of the influence of the factor x_3 on the functioning of the exciter is confirmed by the regulation characteristics, Fig. 4. Experiments within each pair (1, 5;

2, 6; 3, 7; 4, 8) were carried out for different values of x_3, while the characteristics do not differ significantly from each other in pairs. In contrast to the significant difference in $C_\Sigma(\zeta)$ between the specified pairs of experiments. The predominant influence of the factor x_1 over x_2 is confirmed by a larger number of steps for the curves of the pair of experiments 2, 6 compared to the corresponding experiments of the pair 3, 7 at the same pairwise values of C_{max}. When numbering the states of the exciter in ascending order by C_Σ, as is done in Fig. 4, the regulating characteristic of the exciter is an increasing significantly nonlinear curve. The increase in the total capacitance is accompanied by an increase in the intensity of its growth. The step characteristics, Fig. 5, indicate a predominant number of steps close to the δ_{min} value. In particular, for experiment 8, 16000 steps with a value of $\delta < 3 \cdot 10^{-3}$ % (at $\delta_{min} = 5.1 \cdot 10^{-4}$ %), which is 88 % of $H_8 = 18209$, were recorded. This confirms the main hypothesis of the study, since the possibility of minimizing the relative value of mean $\overline{\delta}$ of the changing step of the exciter capacitance is confirmed. In particular, for experiments 2, 4, 6, 8, 9, condition (3) is satisfied, since $\overline{\delta} < 0.2$ %, Table 4. That is, by choosing an exciter configuration with a variable topology, it is possible to reduce the changing step of the total capacitance to meet the requirements.

Compared with the method [25] of controlling an autonomous IG by using a ballast load with PWM regulation, the proposed scheme of a capacitor exciter with a variable topology is characterized by economy. The ballast load dissipates part of the active energy generated. At the same time, the regulated exciter changes the magnetization conditions of the generator, which allows stabilizing the output voltage parameters. Compared with the use of compound capacitors [15], the proposed exciter scheme does not provide for the flow of operating current through the capacitors. This increases the reliability and stability of the functioning of the autonomous generator. The implementation of a variable exciter topology, when mixed connections of capacitors are used in various combinations, significantly increases the number of adjustment steps compared to the classical method of using several capacitor banks [26]. When using 8 triac-switched capacitors [27], when their parallel connection is implemented in each phase, it is possible to obtain only $2^{8-1} = 128$ adjustment steps of the total exciter capacitance. At the same time, as follows from Table 4, the proposed method allows to obtain 183 (experiment 3), 278 (experiment 7), 518 (experiment 2) or 796 (experiment 6) adjustment steps. In this case, a similar number of capacitors is used. This is 1.4, 2.2, 4 and 6.2 times more than in the known method [27], respectively. The specific number of steps is determined by the connection method and the degree of change in the capacitance of adjacent capacitors.

The possibilities of regulating the exciter capacitance, which illustrate the characteristics in Fig. 4, 5, are due to the use of a flexible structure. The implementation of a mixed connection of capacitors makes it possible to minimize the step change in the total capacitance. For example, for the conditions of experiment 8, such an indicator with a probability of 0.88 does not exceed $3 \cdot 10^{-3}$ % of the width of the regulation range. The use of an exciter with a variable topology as part of an autonomous IG allows to solve the existing problem. Namely, to increase the efficiency of controlling the excitation level of an autonomous induction generator when changing the speed of the drive turbine and the load impedance. The efficiency increases by increasing the number of regulation stages, which raises the accuracy of forming the capacitive excitation current of the IG and compensating the inductive component of the load current. Accordingly, the quality indicators of the generator output voltage will increase, and fluctuations in the amplitude and frequency of the output voltage will be reduced. This will increase the quality of power supply for the functioning of consumers as part of an autonomous electric network. The proposed exciter with variable topology can be used as part of self-excited induction generators, including dual star induction generator, as part of autonomous power supply systems and microgrids.

The limitations of the above study include the failure to consider transients that accompany a change in the exciter configuration when it is necessary to change the total capacitance. The duration and nature of transients can in some way affect the generator voltage regulation time.

The disadvantages of the proposed approach to excitation of an induction generator include the need to use high-speed switching devices for switching capacitors. In the exciter circuit, overvoltages may occur during switching, which must be taken into account when building a generator protection system.

In the course of further research, it is planned to investigate, theoretically and experimentally, the functioning of an autonomous induction generator with the proposed variable topology exciter. This will allow numerically assessing the improvement in the quality of regulation of the generator output voltage under the influence of external disturbances.

7. Conclusions

1. As a result of the evaluation of the parameters values of the capacitor exciter mathematical model, the significance of the influence of the groups number and the number of capacitors in each group on the width of the range and the adjustment step was confirmed. In particular, an increase in the values of the specified factors from 2 to 4 expands the adjustment range by 16 times (from 12 μF to 195 μF), and the number of steps – by 827 times (from 22 to 18209). The influence of each of the specified factors on the mean of the relative value of the step change in the exciter capacitance prevails over the influence of their interaction, which is taken into account by the product. At the selected intervals of factors variation and the significance level of 0.05, the influence of the degree of change in the capacitance of the circuit capacitors, compared to the base, on the relative value of the step change in the exciter capacitance is recognized as insignificant. The resulting regression mathematical model can be used in optimizing the exciter structure for an autonomous induction generator of a specific type.

2. The total capacitance of the proposed exciter depends significantly nonlinearly on the topological state number. For configurations from 2 to 4 groups with a number of capacitors from 2 to 4, about 98 % of discrete states cover 20 % of the total exciter capacitance, the remaining 2 % – 80 %. The increase in the total capacitance is accompanied by intensity rise of its growth. This is explained by the use of a mixed connection of capacitors. The advantages of this method, compared to the known method of using only parallel capacitors, include minimizing the step change in the total capacitance (with a probability of 0.88 – up to $3 \cdot 10^{-3}$ % of the width of the adjustment range). Increasing the number of adjustment stages will allow to increase the accuracy of the

formation of the capacitive excitation current of the generator and compensation of the inductive component of the load current. Thus, it will be possible to increase the efficiency of controlling the excitation level of an autonomous induction generator when changing the speed of the drive turbine and the load impedance.

Conflict of interest

The authors declare that they have no conflict of interest in relation to this research, whether financial, personal, authorship or otherwise, that could affect the research and its results presented in this paper.

Financing

The study was conducted without financial support.

Data availability

The manuscript has no associated data.

Use of artificial intelligence

The authors confirm that they did not use artificial intelligence technologies when creating the current work.

References

1. Communication From The Commission To The European Parliament, The European Council, The Council, The European Economic And Social Committee And The Committee Of The Regions (2019). European Commission. Available at: https://eur-lex.europa.eu/resource.html?uri=cellar:b828d165-1c22-11ea-8c1f-01aa75ed71a1.0002.02/DOC_1&format=PDF
2. Allen, M. R., Friedlingstein, P., Girardin, C. A. J., Jenkins, S., Malhi, Y., Mitchell-Larson, E. et al. (2022). Net Zero: Science, Origins, and Implications. Annual Review of Environment and Resources, 47 (1), 849–887. https://doi.org/10.1146/annurev-environ-112320-105050
3. Communication From The Commission To The European Parliament, The European Council, The Council, The European Economic And Social Committee And The Committee Of The Regions (2022). European Commission. Available at: https://eur-lex.europa.eu/resource.html?uri=cellar:fc930f14-d7ae-11ec-a95f-01aa75ed71a1.0001.02/DOC_1&format=PDF
4. Communication From The Commission To The European Parliament, The Council, The European Economic And Social Committee And The Committee Of The Regions (2022). European Commission. Available at: https://eur-lex.europa.eu/legal-content/EN/TXT/PDF/?uri=CELEX:52022DC0552
5. Renewables 2024. Analysis and forecasts to 2030. International Energy Agency. Available at: https://www.iea.org/reports/renewables-2024
6. Global wind report 2024. Global Wind Energy Council. Available at: https://img.saurenergy.com/2024/05/gwr-2024_digital-version_final-1-compressed.pdf
7. Andrienko, D., Horiunov, D., Hrudova, V., Markuts, Yu., Marsholok, T., Neiter, T. et al. (2025). Zvit pro priami zbytky infrastruktury vid ruinuvan vnaslidok viyskovoi ahresiyi Rosiyi proty Ukrainy stanom na lystopad 2024 roku. Available at: https://kse.ua/wp-content/uploads/2025/02/KSE_Damages_Report-November-2024-UA.pdf
8. Pro skhvalennia Enerhetychnoi stratehiyi Ukrainy na period do 2050 roku. Rozporiadzhennia Kabinetu Ministriv Ukrainy No. 373-r. Available at: https://zakon.rada.gov.ua/laws/show/373-2023-%D1%80#Text
9. Alhusein, N. I. (2022). Asynchronous Wind Turbine Generator: Output Power Evaluation. Brilliance: Research of Artificial Intelligence, 1 (2), 75–80. https://doi.org/10.47709/brilliance.v1i2.1565
10. Induction Generators Market (2025). Verified Market Reports. Available at: https://www.verifiedmarketreports.com/select-license/?rid=484938
11. Li, H., Peng, W., Huang, C.-G., Guedes Soares, C. (2022). Failure Rate Assessment for Onshore and Floating Offshore Wind Turbines. Journal of Marine Science and Engineering, 10 (12), 1965. https://doi.org/10.3390/jmse10121965
12. Alizadeh, A., Kamwa, I., Moeini, A., Mohseni-Bonab, S. M. (2023). Energy management in microgrids using transactive energy control concept under high penetration of Renewables; A survey and case study. Renewable and Sustainable Energy Reviews, 176, 113161. https://doi.org/10.1016/j.rser.2023.113161
13. Mahato, S. N., Singh, S. P., Sharma, M. P. (2008). Excitation capacitance required for self excited single phase induction generator using three phase machine. Energy Conversion and Management, 49 (5), 1126–1133. https://doi.org/10.1016/j.enconman.2007.09.007
14. Goyal, S. K., Palwalia, D. K. (2016). Analysis of performance parameters and estimation of optimum capacitance for asynchronous generator. Engineering Science and Technology, an International Journal, 19 (4), 1753–1762. https://doi.org/10.1016/j.jestch.2016.05.015
15. Khan, M. F., Khan, M. R., Iqbal, A. (2022). Effects of induction machine parameters on its performance as a standalone self excited induction generator. Energy Reports, 8, 2302–2313. https://doi.org/10.1016/j.egyr.2022.01.023
16. Negi, G. S., Gupta, M. K., Saxena, N. K., Mohan, H. (2024). Squirrel cage induction generator based micro grid voltage assessment with STATCOM using different metaheuristic approaches. E-Prime - Advances in Electrical Engineering, Electronics and Energy, 9, 100736. https://doi.org/10.1016/j.prime.2024.100736
17. Guettab, A., Boudjema, Z., Bounadja, E., Taleb, R. (2022). Improved control scheme of a dual star induction generator integrated in a wind turbine system in normal and open-phase fault mode. Energy Reports, 8, 6866–6875. https://doi.org/10.1016/j.egyr.2022.05.048
18. Belalia, K., Mostefa, A., Merabet Boulouiha, H., Draou, A., Denai, M. (2024). Direct torque control of a dual star induction generator based on a modified space vector PWM under fault conditions. ISA Transactions, 155, 237–260. https://doi.org/10.1016/j.isatra.2024.10.012

19. Milles, A., Merabet, E., Benbouhenni, H., Debdouche, N., Colak, I. (2024). Robust control technique for wind turbine system with interval type-2 fuzzy strategy on a dual star induction generator. Energy Reports, 11, 2715–2736. https://doi.org/10.1016/j.egyr.2024.01.060
20. Benbouhenni, H., Bizon, N., Colak, I., Mosaad, M. I., Yessef, M. (2023). Direct active and reactive powers control of double-powered asynchronous generators in multi-rotor wind power systems using modified synergetic control. Energy Reports, 10, 4286–4301. https://doi.org/10.1016/j.egyr.2023.10.085
21. Gu, T., Wang, P., Liu, D., Sun, A., Yang, D., Yan, G. (2023). Modeling and small-signal stability analysis of doubly-fed induction generator integrated system. Global Energy Interconnection, 6 (4), 438–449. https://doi.org/10.1016/j.gloei.2023.08.005
22. Zhao, T., Liu, H., Luo, Z., Su, Y., Huang, L., Li, H., Sun, Z. (2023). A frequency control scheme of a doubly-fed induction generator considering random wind speeds. Energy Reports, 9, 235–244. https://doi.org/10.1016/j.egyr.2023.04.101
23. Mostafavi, S., Shemshadi, A., Nazari, R., Yousefkhani, H. (2025). Utilization of H∞ robust and damping controllers with notch filters to reduce SSR in doubly-fed induction generator wind farms. Computers and Electrical Engineering, 123, 110024. https://doi.org/10.1016/j.compeleceng.2024.110024
24. Cheng, C.-L., Shalabh, Garg, G. (2014). Coefficient of determination for multiple measurement error models. Journal of Multivariate Analysis, 126, 137–152. https://doi.org/10.1016/j.jmva.2014.01.006
25. Reddy, S. R. K. (2021). Review of Literature on Self-Excited Induction Generators and Controllers. International Journal for Research in Applied Science and Engineering Technology, 9 (12), 1576–1587. https://doi.org/10.22214/ijraset.2021.39584
26. Mykhailiuk, O. B. (2016). Problems that need a solution while using asynchronous generator of renewable energy in power plants. Visnyk of Vinnytsia Polytechnical Institute. Visnyk Vinnytskoho politekhnichnoho instytutu, 1, 96–100. Available at: https://visnyk.vntu.edu.ua/index.php/visnyk/article/view/1883
27. Pushkar, M., Buryan, S., Mykhailenko, V. (2014). The voltage regulation of self-excited induction generator with triac-switched capacitor bank. Pratsi Instytutu elektrodynamiky Natsionalnoi akademiyi nauk Ukrainy, 39, 52–56. Available at: http://nbuv.gov.ua/UJRN/PIED_2014_39_11